

REFRACTIVITY MEASUREMENTS FROM GROUND CLUTTER USING THE NATIONAL WEATHER RADAR TESTBED PHASED ARRAY RADAR

B. L. Cheong^{1,*}, R. D. Palmer¹, T.-Y. Yu² and C. Curtis³

¹School of Meteorology, University of Oklahoma, Norman, U.S.A.

²School of Electrical and Computer Engineering, University of Oklahoma, Norman, U.S.A.

³Cooperative Institute of Mesoscale Meteorological Studies (CIMMS), The University of Oklahoma and NOAA/OAR National Severe Storms Laboratory

1. INTRODUCTION

Small-scale/regional weather forecasts rely on surface water vapor profiles which is directly related to convective precipitation initiation [e.g., Hanssen et al., 1999; Mohan et al., 2001]. For instance, a necessary condition for an accurate prediction of convective rainfall is a good forecast of where and when convection will develop. Both prediction and understanding of convection is limited at this time due to the lack of high spatial and temporal resolution of water vapor measurements [Weckwerth and Parsons, 2003]. Radiosondes that launch twice a day simply do not supply the measurements at the desired level of temporal and spatial resolution. Besides, GPS measurements do not provide sufficient vertical resolution for the small-scale studies and the measurements near the surface are not reliable [Braun, 2001]. Near surface measurements were deemed necessary but it is very expensive to implement a dense network of data acquisition stations to achieve this goal.

A more attractive approach is to use some kind of remote sensing near the surface. Pioneering work that uses ground targets to measure refractivity, which is closely related to humidity, has been accomplished by Fabry et al. [1997]. Initial experiments were conducted in Montreal, Canada and demonstrated promising potential [Fabry et al., 1997; Fabry and Creese, 1999]. In addition, extensive experiments were conducted during the International H₂O Project 2000 (IHOP_2000) campaign [Fabry and Pettet, 2002; Weckwerth and Parsons, 2003]. The key is that refractivity can be obtained by measuring the phase of radar echoes.

The phase of radar backscattered echoes depends on the electromagnetic characteristics of the targets, the motions of the targets and the atmospheric conditions in

which the radio waves propagate. For echoes that are reflected from perfectly stationary targets, the phase of the received signal is constant assuming the refractivity of the air mass between the radar and the target remains unchanged. Temporal variations in humidity and temperature can cause subtle, yet measurable, phase changes in the backscattered signal.

In this brief article, preliminary results of refractivity mapping using a phased array radar with a temporal resolution of 6 s will be presented. The raw datasets were collected using the S-band Phased Array Radar (PAR), which is the centerpiece of the National Weather Radar Testbed (NWRT) located in Norman, Oklahoma and is operated by the National Severe Storms Laboratory (NSSL). Here, we will investigate the advantages of the use of a phased array radar system. Possible advantages of the use of phased array technology may be the mitigation of smearing of clutter targets due to antenna motion, adaptive mapping of clutter targets, and rapid update times, for example.

2. THE PHASED ARRAY RADAR

Navy AN/SPY-1A technology used in weaponry [Sensi, 1988] has been adopted for meteorological research at NSSL. The system is also referred to as the PAR system in the NWRT of the NSSL. The PAR system operates at the 3.2 GHz S-band and uses a standard WSR-88D transmitter, an array of 4352 receivers and a flexible data acquisition system. It uses real-time beamforming to probe the atmosphere for weather conditions and collects raw in-phase and quadrature time-series from the analog beamformer. At the present time, time-series can be processed in real-time and simultaneously stored for off-line processing. One of the attractive features of the PAR system is the mitigation of image-smearing effects that are inherent in the standard WSR-88D due to antenna motion. In the PAR system, however, this smearing effect is eliminated since the beams of the PAR are fixed without any antenna rotation. In addition,

* *Corresponding author address:* Boon Leng Cheong, University of Oklahoma, School of Meteorology, 100 East Boyd Street, Suite 1310, Norman, OK 73019; e-mail: boonleng@ou.edu

agile beam steering is yet to be exploited in this technology for remote sensing of the atmosphere.

3. REFRACTIVITY MEASUREMENTS

3.1. Basics of Refractive Index and Radio Waves

Refractive index, n , of a medium is the ratio of the speed of light in a vacuum to the speed of light in the medium. For the air near the surface of the earth, this number is typically around 1.003 and changes of this number are on the order of 10^{-5} [Bean and Dutton, 1968]. For convenience, a derived quantity referred to as refractivity is used in many scientific studies. The *refractivity* is described as follows

$$N = 10^6(n - 1) \quad (1)$$

and this function is related to meteorological parameters as follows [Bean and Dutton, 1968]

$$N = 77.6 \frac{p}{T} + 3.73 \times 10^5 \frac{e}{T^2} \quad (2)$$

where p represents the air pressure in millibar (mb), T represents the absolute air temperature in Kelvin (K) and e represents the vapor pressure in mb. The first term in Equation (2) is proportional to pressure p that is related to the air density; the second term is proportional to vapor pressure e and is mainly contributed by the water content in the air. The two terms can be referred to as dry and wet terms, respectively. Near the surface of the earth with relatively warm temperature, most of the spatial variability in N results from the change in the second term. For example, a change of 1 N -unit (10^{-6} in n) can result from a change of 1 °C in temperature or 0.2 mb in vapor pressure under a nominal condition of $p = 1000$ mb and air temperature at 27 °C.

Quantitatively, given an average pressure and temperature over the radar coverage, humidity is expected to be estimated with reasonable accuracy. At a fixed air pressure, say a typical surface pressure around 1000 mb, refractivity N becomes a function of e and T and is depicted in Figure 1. As temperature increases, refractivity change becomes more sensitive to vapor pressure (humidity) than to temperature and pressure. One can readily see that vapor pressure e is the dominant factor that changes the refractivity and thus refractivity mapping near the surface can be used as a proxy to estimate the spatial distribution of water vapor near the surface [Fabry et al., 1997].

In the free space vacuum, radio wave propagates at the speed of light. In the atmosphere that contains all

the constituent gases and water vapor, its propagation speed is slowed down depending on the refractivity resulting from these various contents. In fact, its speed is an inverse function of refractive index. The time for a radio wave to propagate to a stationary target and come back through a constant refractivity medium is [Fabry et al., 1997]

$$t_{\text{travel}} = 2r \frac{n}{c} \quad (3)$$

where r is the radial distance from the radar to the target and c is the speed of light in vacuum ($299,792,458 \text{ m s}^{-1}$). For most radar applications, effects of n can be safely neglected since it varies by at most 0.03%. Changes at this scale do not affect most applications because the change of phase of the radio waves is dominated by the velocity of targets. For our interest, however, ground targets are completely stationary and thus the only factor that contributes to the change of phase is the refractivity function of the two-way path. By including the variations of the refractive index n along the two-way path defined in Equation (3), the phase of the returned radio wave is

$$\phi(r) = 2\pi f t_{\text{travel}} = \frac{4\pi f}{c} \int_0^r n(\gamma) d\gamma \quad (4)$$

One point must be made clear before this fundamental formulation is exploited, i.e., the phase measurement at the radar receiver contains the *integrated* (not at the particular position) refractive index along the two-way path in which the radio wave has traveled, assuming the target is completely stationary.

As mentioned before, the propagation speed of the radio wave is slowed down due to the refractivity along the two-way path. The changes of the refractivity cause the phase of the returned echoes to change as the travel time changes (Refer Equation (3)). Figure 2 illustrates an example of phase measurements of ground targets from four distinct range gates. One can see that the phase of the returned echoes from good ground targets changes slowly over time, which may be caused by change of temperature T , pressure P or vapor pressure e . For ground targets that are not completely stationary, the phase measurements are noisy (e.g., Gate #55).

For an area with sufficient ground target coverage, which is often the case within the radius of approximately 30 km from the radar, the refractivity can be mapped within a spatial resolution on the order of a few km [Fabry and Pettet, 2002]. One might be concerned that refractivity changes along the two-way path might bend the radio wave if extended range is considered. A direct calculation by applying Snell's Law tells us that an integrated change of refractivity of 150 N -unit is needed in order to bend the radio wave by 1°. Since refractive

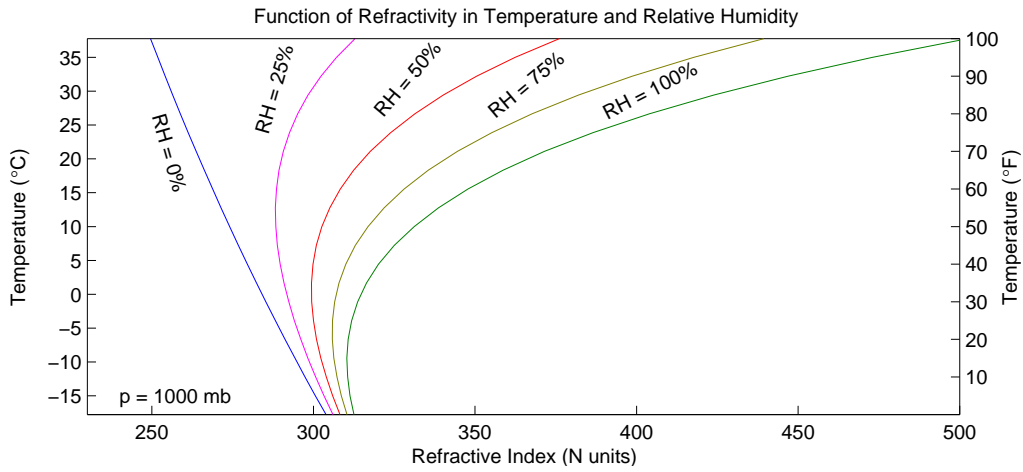


Figure 1: Refractivity N as a function of temperature T and relative humidity (derived from T and e). At a surface pressure of 1000 mb and temperature above 10°C , refractive index changes predominantly based on the relative humidity (vapor pressure). As temperature increases, N becomes more sensitive to the change of e and thus can be used as a proxy to estimate the water vapor near the surface. This method may be very useful especially during warm seasons.

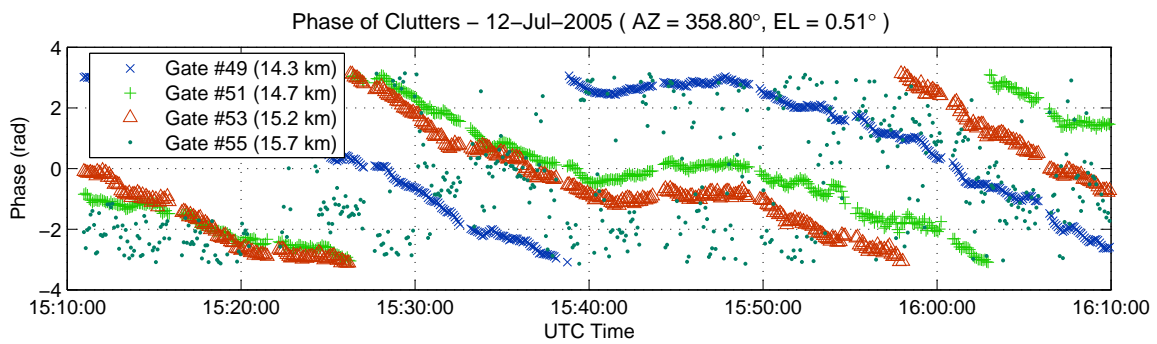


Figure 2: Example of phase measurement of ground clutter. For good clutter, the phase changes steadily as shown in the figure, due to atmospheric changes. If there is no change in the atmospheric condition, the phase remains constant.

index is only expected to change on the order of 10 N -units, path bending effects can be safely ignored for an angular scan of every 1° .

3.2. Phase Measurement

Refractivity mapping near the surface using radar echoes from ground targets was first conducted by Fabry et al. [1997]. The method relies on the phase measurement of the returned radio waves to estimate the refractivity map. Because the wavelength of the S-band is very short (approximately 10 cm), the integrated refractivity induces an extremely quick phase wrap for this wavelength which is problematic. One way around this is by looking at the change of phase at two time instances. Doing so is equivalent to applying Equation (4) twice at two different times, say at time t_0 and t_1 , the phase difference between the two observations can be described as

$$\begin{aligned}\Delta\phi(r) &= \phi(r, t_1) - \phi(r, t_0) \\ &= \frac{4\pi f}{c} \int_0^r [n(\gamma, t_1) - n(\gamma, t_0)] d\gamma. \quad (5)\end{aligned}$$

Usually the measurement at time t_0 is used as a reference phase map. A good reference map is a map obtained during a time when spatial distribution of the refractivity is homogeneous. As suggested by Fabry [2004], a reference phase is best to be measured immediately after several hours of stratiform precipitation, preferably in a windy condition and cool temperatures. The reasons being: (i) wind helps homogenize the humidity field of the region; and (ii) cool temperature narrows down the range of the refractivity.

Once a reference map is available, and from Equation (5), we have

$$\frac{d}{dr} [\phi(r, t) - \phi_{\text{ref}}(r)] = \frac{4\pi f}{c} [n(r, t) - n_{\text{ref}}(r)], \quad (6)$$

where $\phi_{\text{ref}}(r)$ and n_{ref} is the phase and refractive index at the time of reference, respectively. Using Equation (6), one can determine n over a short path and avoid the phase-wrap problem as mentioned previously.

In order to obtain the change of refractivity in N -units, Equation (5) is reversed by applying the derivative operator on both sides.

$$\begin{aligned}\Delta N &= 10^6 [n(r, t) - n_{\text{ref}}(r)] \\ &= 10^6 \frac{c}{4\pi f} \frac{d}{dr} [\phi(r, t) - \phi_{\text{ref}}(r)] \quad (7)\end{aligned}$$

4. EXPERIMENTAL RESULTS

A 1-hour dataset was collected using the PAR system at an elevation angle of 0.51° , with the antenna of the PAR facing north, obtaining a 90° azimuthal scan from -45° to $+44^\circ$ (1° spacing). The system was set to have a pulse repetition time (PRT) of 1 ms, a dwell of 64 pulses resulting in a temporal resolution of approximately 6 s. Figure 3 shows an average signal-to-noise ratio (SNR) map over the 1-hour period. Within the first 30 km of the radar coverage, ground clutter can be seen in the SNR map. The datasets were collected when no significant atmospheric phenomena were present. With proper power calibration, reflectivity in dBZ can be derived and is shown in the upper right panel. Not all ground targets should be used for refractivity mapping and a measure of the quality must be determined. At this point, a 2-min (lag-20) correlation coefficient of the phase is used to determine the quality of ground clutter. The lower-left panel shows the 2-min-lag correlation coefficient of the phase of the returned echoes. It can be seen that the curved returns in the SNR map, which could be created by flying aircraft are no longer seen because they have poor phase correlation. Gridded structures within close range can be seen in the quality index map indicating building structures along streets. Within the 1-hour dataset, the first 10-min subset is used to derive a reference phase map, in which the phase values are obtained by computing the average of the signal phase over the 10-min period. Reference refractivity values are obtained using the atmospheric measurements from the surrounding Mesonet surface stations.

After obtaining the clutter quality index map, phase measurements are extracted based on the quality index for refractivity mapping. Figure 4 demonstrates a phase measurement that masks everything except good clutter. The left panel shows the phase difference of the snapshot from the reference phase, which is the value of Equation (5). A slow phase wrap can be seen as a consequence of the phase measurements containing the *integrated* refractivity. In order to compute the radial derivatives of the phase change, a smoothing/patching operation is applied to obtain the continuous phase difference. The technique being used here closely mimics the algorithm of up-sampling in which signals are first zero-padded, then a low-pass filter (smoothing window) is applied for smoothing and interpolation. For our case, the regions with low quality index are set to zero (zero-padded) and the rest are set to $e^{i\Delta\phi}$ (original signals). Then, the map is smoothed (filtering) using a 2-D convolution with a Gaussian window function, in which the width of the window function is set to be 4 km. For each range gate, a different smoothing window function is ap-

12-Jul-2005 16:06:28 UTC (EL = 0.51°)

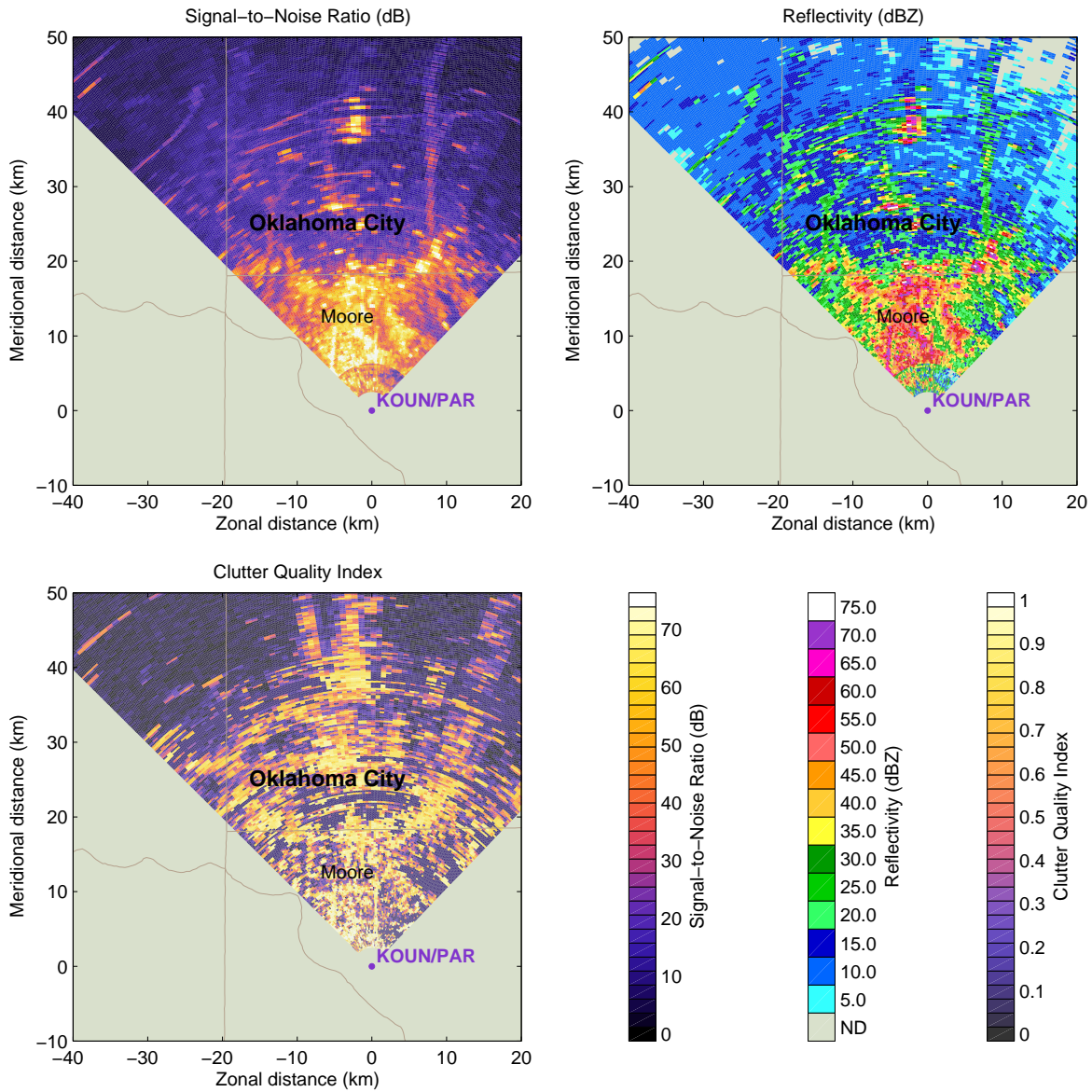


Figure 3: Clutter quality index is obtained by computing the 2-min-lag correlation coefficients of the phase of the returned echoes. For perfectly stationary targets, the phase is expected to be similar and thus have values closer to 1. On the other hand, non-stationary targets do not return similar phase and thus have values closer to 0.

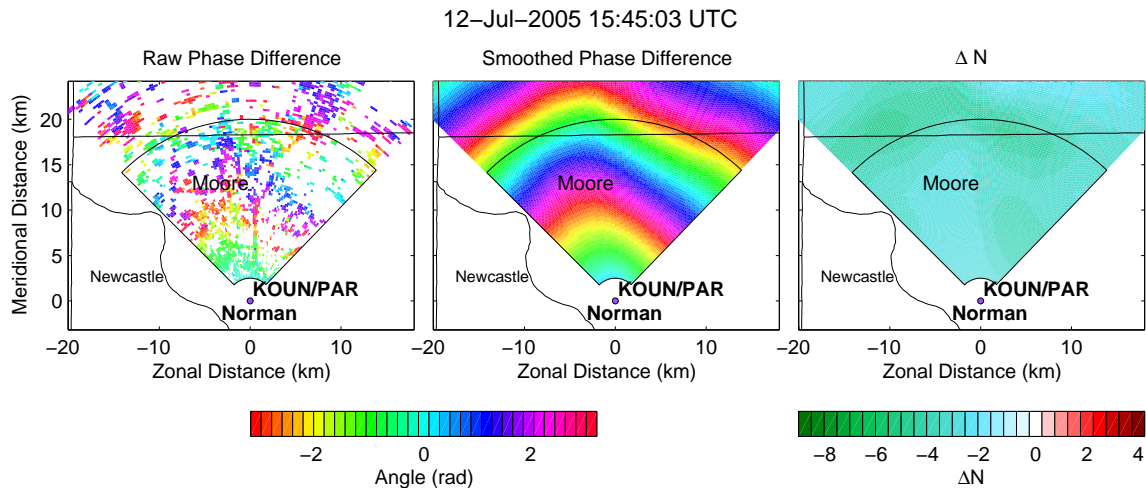


Figure 4: Change of Refractivity can be obtained from the gradient along the range of the phase differences (refer to Equation (7)).

plied in order to maintain the 4-km width. For each azimuth, a same smoothing window function (4-km width) is applied along the radial dimension through the entire map. The middle panel shows the continuous version of the left panel. Equation (7) is applied to the middle panel to find the change of refractivity ΔN and the result is shown in the right panel. Absolute refractivity N can be found by adding back the reference refractivity. At the present time, however, only ΔN is found as this algorithm is efficient in detecting the change of refractivity.

After processing the entire 1-hour dataset, slow variations in refractivity can be seen when the processed datasets are animated. Figure 5 shows several snapshots of the change of refractivity (using the first 10-min dataset as a reference). A general trend of negative change in the refractivity can be seen in this dataset. The change of refractivity (with much coarser spatial and temporal resolution) can also be obtained from the Oklahoma Mesonet stations surrounding the PAR system. Figure 6 shows an example of standard measurements that are obtained from the Mesonet. The Mesonet data are available at a temporal resolution 5 min. By collecting all the parameters for the refractivity function in Equation (2), a map of refractivity can be obtained. For the sake of comparison, we use refractivity maps obtained from the Mesonet to derive another version of the change of refractivity during that 1-hour period.

We compute the average of three refractivity maps at 15:10, 15:15 and 15:20 UTC to be the reference refractivity map. This is the same time period in which the reference map was computed for the PAR system.

Then, the change of refractivity can be obtained for every 5 min in the Mesonet dataset. Figure 7 shows the change of refractivity obtained using the dataset from the Mesonet. Comparing Figures 5 and 7, a general negative trend in refractivity can be seen in both results, validating the algorithm for refractivity retrieval through phase measurements. In the future, more meteorologically interesting datasets will be collected (e.g., dry line, frontal passage), in order to facilitate the validation of this refractivity retrieval algorithm.

5. CONCLUSIONS

Mapping of refractivity using phase measurements of the ground clutter has been successfully implemented using the PAR system of the NWRT. For refractivity mapping, ground clutter becomes useful as opposed to being treated as a contaminant in most weather observations. Phase measurements from the ground clutter contain information of refractivity, and the work by Fabry et al. [1997] has proven the usefulness of deriving refractivity maps using the phase measurements of ground clutter. Similar algorithms were used for the present work and preliminary results demonstrate promising potential of the algorithm with the PAR system. Future work includes a more thorough validation of the algorithm and statistical analysis on the performance of the system. Theoretical limits of the algorithm have yet to be found and this may be a potential topic to be pursued in the future.

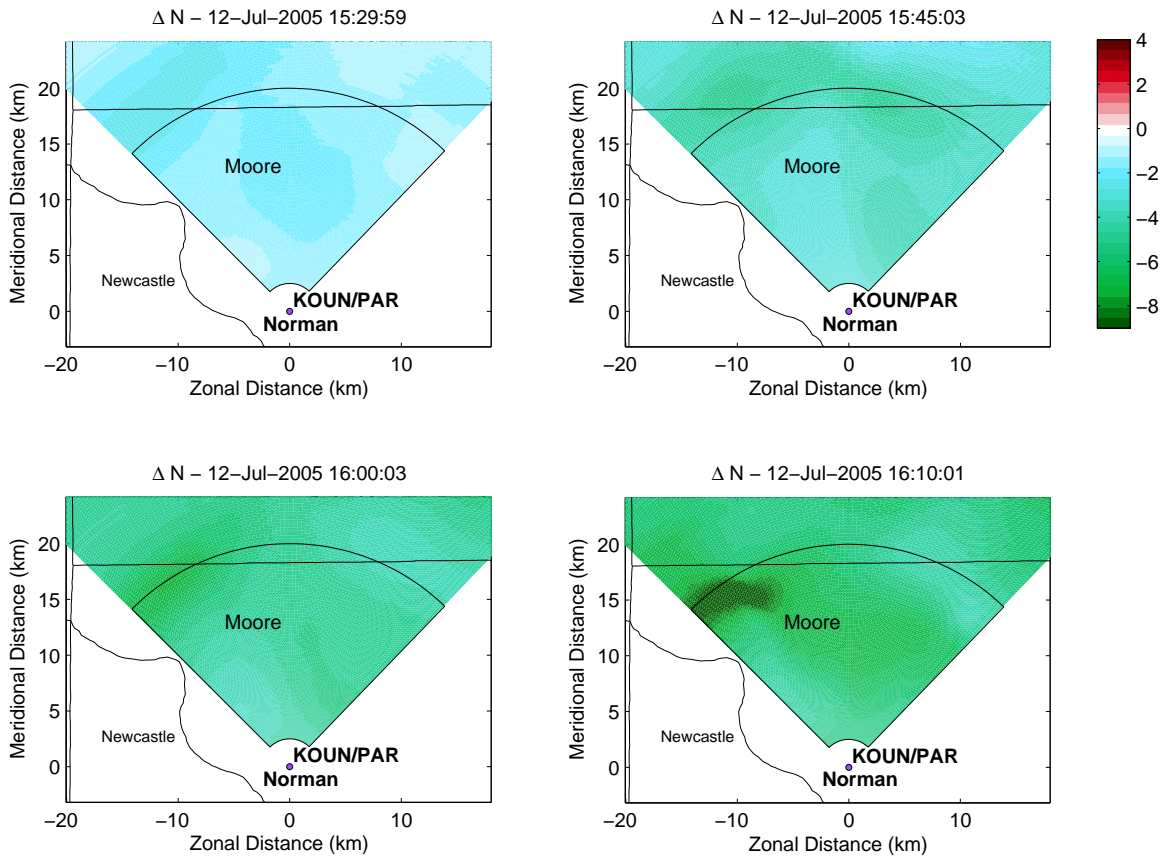


Figure 5: Temporal change of refractivity derived from phase measurement acquired by the PAR. Over the 1-hour period, a generic trend of negative change in refractivity is observed which is somewhat consistent with measurements obtained from the Oklahoma Mesonet.

Mesonet 12-Jul-2005 16:30 UTC

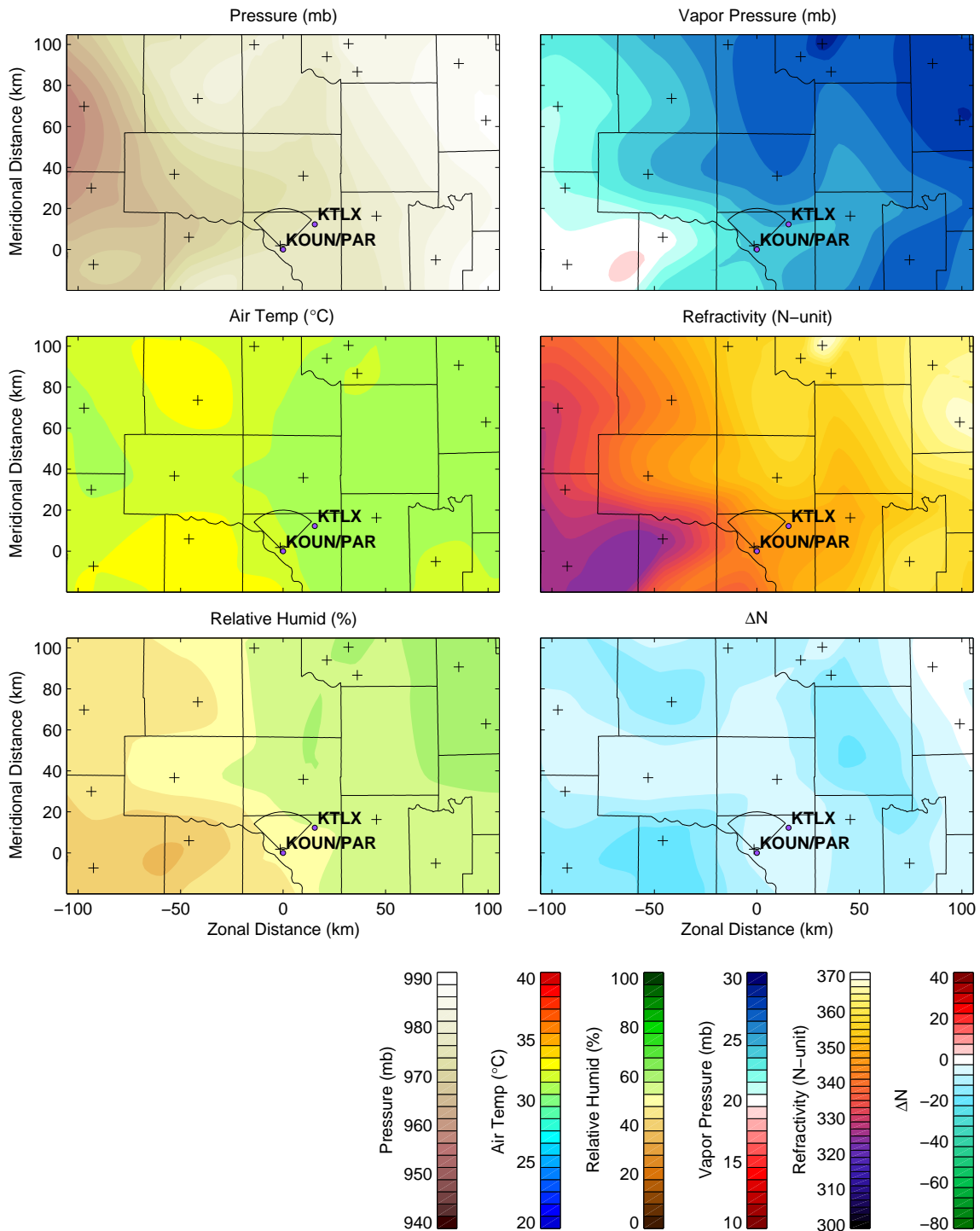


Figure 6: Example of Mesonet Data. Closely spaced weather stations provide meteorological measurements every 5 min. Some of these parameters can be used to derive refractivity maps in order to verify the results obtained from the PAR system.

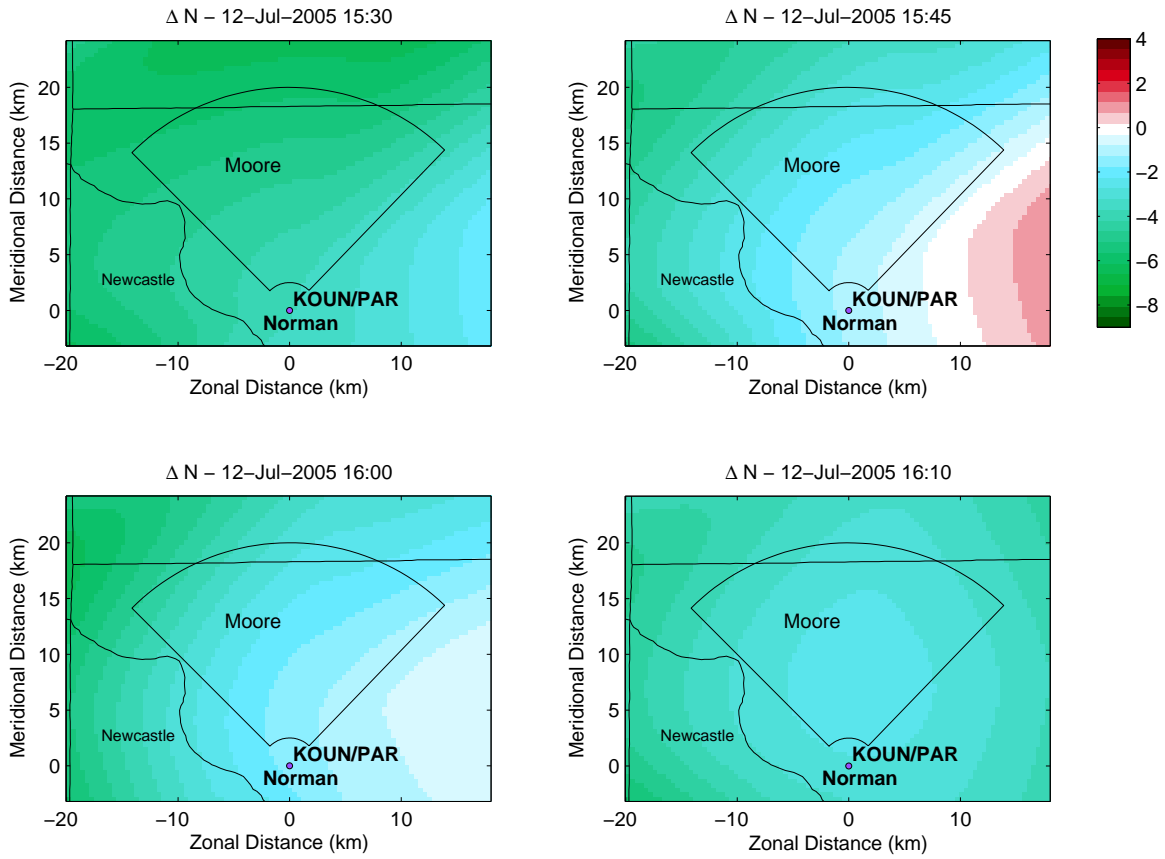


Figure 7: Temporal change of refractivity derived from weather measurements (p , T and relative humidity), which are obtained from Mesonet data every 5 min. Even with significant fluctuation of refractivity (due to fluctuation in humidity measurements) obtained through Mesonet dataset, a general trend of negative change in refractivity can be seen in this 1-hour dataset.

References

- Bean, B. R., and E. J. Dutton, 1968: *Radio Meteorology*. Dover Publications.
- Braun, J., 2001: Validation of a line-of-sight water vapor measurement with GPS. *Radio Sci.*, **36**(3), 459–472.
- Fabry, F., 2004: Meteorological value of ground target measurements by radar. *J. Atmos. Oceanic Technol.*, **21**(4), 560–573.
- Fabry, F., and C. Creese, 1999: If fine lines fail, try ground targets. *Preprints, 29th Conf. on Radar Meteorology, Montreal, Canada, Amer. Meteor. Soc.*, pp. 21–23.
- Fabry, F., C. Frush, I. Zawadzki, and A. Kilambi, 1997: On the extraction of near-surface index of refraction using radar phase measurements from ground targets. *J. Atmos. Oceanic Technol.*, **14**(14), 978–987.
- Fabry, F., and C. Pettet, 2002: A primer to the interpretation of refractivity imagery during IHOP_2002. *IHOP_2002 Refractivity Manual*.
- Hanssen, R. F., T. M. Weckwerth, H. A. Zebker, and R. Klees, 1999: High resolution water vapor mapping from interferometric radar measurements. *Science*, **283**, 1297–1299.
- Mohan, K., D. N. Rao, T. N. Rao, and S. Raghavan, 2001: Estimation of temperature and humidity from MST radar observations. *Annales Geophysicae.*, **19**, 855–861.
- Sensi, Jr., J., 1988: The AEGIS system. in *Aspects of Modern Radars*, pp. 239–277. Artech House.
- Weckwerth, T. M., and D. B. Parsons, 2003: An overview of the international H₂O project (IHOP_2002). *Bull. Amer. Meteor. Soc.*, **85**(2), 253–277.